Letters

Effects of Triangular Wave Injection and Current Differential Terms on Multiparameter Identification for PMSM

Qingsong Wang, *Senior Member, IEEE*, Xiaokai Zhao, *Graduate Student Member, IEEE*, Pengfei Yang, Wei Hua, *Senior Member, IEEE*, and Giuseppe Buja, *Life Fellow, IEEE*

***Abstract*—Permanent magnet synchronous motor (PMSM) has been widely used in industry in recent years because of its simple structure, high power density, and high efficiency. Accurate electromagnetic parameters of PMSM are of great significance in many fields, such as control system design, fault diagnosis, and condition monitoring. However, when the motor is in steady-state operation, the traditional identification method will have the issues, such as model accuracy, rank deficient, and the incompletely observable. Therefore, a parameter identification method based on biased triangular wave injection and current differential term is proposed in this article to solve them. In addition, the influence of triangular wave injection and current differential term on motor parameter identification is comparatively analyzed and verified by comparative experiments. Finally, the experimental results show that the proposed method can realize the multiparameter identification of motor resistance, inductance, and flux linkage in steady-state operation.**

***Index Terms*—Current differential term, multiparameter identification, permanent magnet synchronous motor (PMSM), recursive least square (RLS), triangular wave injection.**

I. Introduction

PERMANENT magnet synchronous motor (PMSM) has been widely used in industry in recent years because of its simple structure, high power density, and high efficiency. It is very important to obtain the electromagnetic parameters accurately for the operation and control of the motor, such as control system design, online fault diagnosis, and rotor/stator state monitoring [1], [2]. The parameter identification techniques are usually divided into offline identification methods and online identification methods. Generally, offline identification is performed when the motor is disconnected from the load or at standstill condition, while online identification is performed when the motor is operating with the load connected.

Since the offline parameter identification is performed when the motor is stationary, the method does not waste online control resources [3]. However, the parameters of the motor will be affected by temperature effect and cross saturation, and the error of the offline identification result is larger. The online identification result can be updated in real time, so the identification result is more accurate [4].

At present, the problem of rank deficiency and poor convergence has become a challenge for online identification of motor parameters. So, a full-rank reference/variable model is proposed in [5]. But this method can only identify the resistance and flux linkage rather than the inductance. In [6], the rotor position offset is added as the disturbance signal to solve the rank-deficient problem, but the method can only identify the resistance and flux linkage. A multiparameter estimation scheme for PMSM under variable speed control is proposed in [7]. The method solves the problem of lack of rank by variable speed operation of the motor, but it cannot realize the multiparameter identification in the steady-state operation of the motor. An algorithm based on recursive least square (RLS) is proposed in [8] to solve the problem of rank deficiency and estimate full motor parameters. Furthermore, many scholars combine online parameter identification with position sensorless to improve the performance of position sensorless observation [9], [10], [11], [12]. Zhang et al. [9] proposed a novel pulsewidth modulation current ripple-based online inductance identification method to improve the position estimation accuracy. In order to improve the dynamic performance and robustness of the sensorless control system, the traditional flux sliding-mode observer is modified in [10] by taking the motor parameter variations into consideration. In [11], the online *dq*-axis inductance identification based on high-frequency voltage injection and the resistance identification based on dc voltage injection are integrated into the active flux-based position observer to improve the accuracy of estimated position. In addition, a position sensorless drive and online parameter estimation method for surface-mounted PMSM (SPMSM) based on adaptive full-state feedback current control is proposed in [12] to overcome the rank-deficient and ill-convergence problem.

In this article, a parameter identification method based on triangular wave injection and current differential term is proposed to solve the rank-deficient and ill-convergence problem. First of all, the introduction of current differential term improves the

Manuscript received 29 September 2023; revised 14 November 2023; accepted 3 December 2023. Date of publication 13 December 2023; date of current version 26 January 2024. This work was supported in part by the National Natural Science Foundation of China under Grant 52177171 and in part by Jiangsu Provincial Key Laboratory of Smart Grid Technology and Equipment, Southeast University. *(Corresponding author: Qingsong Wang.)*

Qingsong Wang, Xiaokai Zhao, Pengfei Yang, and Wei Hua are with the School of Electrical Engineering, Southeast University, Nanjing 210096, China, and also with Jiangsu Province Key Laboratory of Smart Grid Equipment and Technology, Nanjing 210096, China (e-mail: qswang@seu.edu.cn; 220213048@seu.edu.cn; 220202944@seu.edu.cn; huawei1978@seu.edu.cn).

Giuseppe Buja is with the Department of Industrial Engineering, University of Padova, 35131 Padova, Italy (e-mail: giuseppe.buja@unipd.it).

Color versions of one or more figures in this article are available at https://doi.org/10.1109/TPEL.2023.3342293.

Digital Object Identifier 10.1109/TPEL.2023.3342293

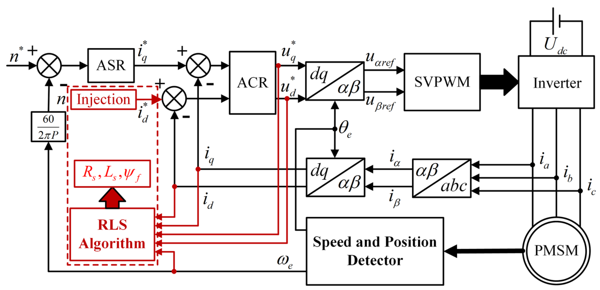

Fig. 1. Block diagram of the parameter identification schemes.

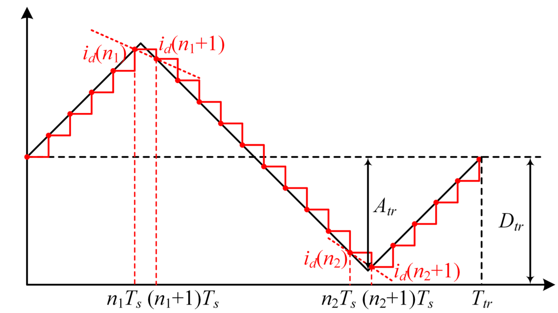

Fig. 2. Diagram of the triangular wave.

accuracy of motor model. Second, the dc offset of the triangle wave increases the signal-to-noise ratio of the stator resistance-related terms. Finally, the identification matrix of the motor is still full rank with the injection of triangle wave with proper amplitude and frequency, so that the resistance, inductance, and flux linkage can be identified successfully.

II. Proposed Method and Analysis

In this section, a detailed introduction is given to the motor parameter identification method based on triangular wave injection and current differential term, including the overall process, triangle wave injection and current differential term introduction methods, and algorithm flow.

A. Overall Process of Parameter Identification

The dynamic model of the PMSM drive in dq frame can be expressed by

$$\begin{cases} u_d = R_s i_d + L_s \frac{di_d}{dt} - \omega_e L_s i_q \\ u_q = R_s i_q + L_s \frac{di_q}{dt} + \omega_e \left(L_s i_d + \psi_f\right) \end{cases} \tag{1}$$

where u_d and u_q are voltages in dq frame, i_d and i_q represent current in dq frame, R_s indicates the stator resistance, ψ_f stands for rotor flux linkage, ω_e is the electrical angular velocity, and L_s indicates the stator inductor (for SPMSM, the d-axis inductance is the same as the q-axis inductance).

In practical applications, due to the fact that the motor identification parameters include resistance, inductance, and magnetic flux, the rank-deficient problem still exists in (1), which means that the identification of three motor parameters cannot be realized by the results of single sampling. Consequently, a new set of equations can be constructed to solve the rank difference problem by using the results of two sampling

$$\begin{cases} u_{d1} = R_s i_{d1} + L_s \frac{di_{d1}}{dt} - \omega_{e1} L_s i_{q1} \\ u_{d2} = R_s i_{d2} + L_s \frac{di_{d2}}{dt} - \omega_{e2} L_s i_{q2} \\ u_{q1} = R_s i_{q1} + L_s \frac{di_{q1}}{dt} + \omega_{e1} (L_s i_{d1} + \psi_f) \\ u_{q2} = R_s i_{q2} + L_s \frac{di_{q2}}{dt} + \omega_{e2} (L_s i_{d2} + \psi_f) \end{cases} \tag{2}$$

where the subscript "1" represents the *nth* sampling result, and the subscript "2" stands the $(n+1)$th sampling result.

Actually, the rank-deficient problem can be solved by choosing any three equations from (2) to form a new system of equations.

The block diagram of parameter identification is shown in Fig. 1. For the control of PMSM driver, the classical field-oriented control is adopted. In the process of motor running, the voltage reference value in dq frame, the current actual value in dq frame, and the electrical angular velocity are sampled first, then they are taken into RLS algorithm for iterative calculation, and finally the value of the resistance, inductance and the flux linkage are obtained.

B. Current Differential Terms and Triangular Wave Injection

In fact, the error caused by the sampling and regulator will result in the deviation of current sampling results, which will lead to the current differential term cannot be regarded as the system noise with the mean value of 0. Therefore, it is necessary to introduce the current differential term into the voltage equations in order to improve the accuracy of the model and reduce the error of the parameter identification results.

However, although (2) solves the rank-deficient problem in terms of the number of equations, it is established on the premise that the motor operation states corresponding to the two sampling points are not consistent. This means that the rank-deficient problem cannot be solved effectively when the motor is running in a steady state because the two sampling points are too close to each other, which may result in the motor parameters cannot be identified successfully. In [8], using the observability theory, it is proved that the motor parameters cannot be completely observed due to the insufficient rank in the steady state of the motor. In order to solve the above problems, triangle wave is injected into the d-axis current to ensure that the two sampling corresponding motor running state is inconsistent enough.

The diagram of the triangular wave is shown in Fig. 2, where $T_{\rm tr}$ represents the period of the triangular wave, $A_{\rm tr}$ represents the amplitude of the triangular wave, and $D_{\rm tr}$ represents the dc offset of the triangular wave. The above three parameters can determine a triangular wave.

The d-axis current differential term after injecting triangular wave has the following characteristics:

$$\begin{cases} \left.\frac{di_d}{dt}\right|_{t=nT_s} = \frac{i_d(n+1)-i_d(n)}{T_s}, n \neq n_1 \text{ and } n_2 \\ \left.\frac{di_d}{dt}\right|_{t=nT_s} \neq \frac{i_d(n+1)-i_d(n)}{T_s}, n = n_1 \text{ or } n_2 \end{cases} \tag{3}$$

where T_s represents the sampling period, $i_d(n+1)$ and $i_d(n)$ stand the $(n+1)$th and nth sampling currents, and n_1 and n_2 denote the previous sampling point closest to the maximum and minimum values of the triangular wave.

From Fig. 2, it can be observed that there is a significant error between the approximate values and the actual values of the current differential terms at sampling points $_1$ and n_2. In order to improve the accuracy of d-axis current differential term approximation, it is necessary to reduce the ratio of sampling point n_1 and n_2 as much as possible. According to Fig. 2, the approximate imprecise points are at most 2. Therefore, it is necessary for the number of sampling points in a triangular wave period to be as large as possible, that is, the sampling period should be much smaller than the triangular wave period.

However, the sampling period cannot be too small; otherwise, the two sets of sampling point data will be too close, which will lead to the recurrence of the rank-deficient problem.

C. Proposed Parameter Identification Method

The RLS algorithm is simple in structure and is widely used, enabling unbiased estimation of the signal with white noise [8]. Consequently, this article adopts two-stage identification algorithm based on RLS to identify the inductance, resistance, and flux linkage of the motor. On the one hand, the reduction of the dimension of the identification matrix will speed up the convergence speed, and on the other hand, the identification frequency of the slowly changing parameters can be reduced, and the controller burden can be further reduced. The steps are described as follows.

Step 1: The triangular wave is injected into the *d*-axis current, and the current differential term is introduced to identify R_s and L_s. The voltage equations used for identification are

$$\begin{cases} u_{d1} = R_s i_{d1} - \omega_{e1} L_s i_{q1} + \frac{L_s}{T_s}(i_{d2} - i_{d1}) + \zeta_1 \\ u_{d2} = R_s i_{d2} - \omega_{e2} L_s i_{q2} + \frac{L_s}{T_s}(i_{d3} - i_{d2}) + \zeta_2 \end{cases} \quad (4)$$

where ζ is a system noise with a mean of 0. According to the RLS algorithm, the identification values of R_s and L_s can be obtained in real time according to the definition of the following formula:

$$\begin{cases} \hat{w}_1(n) = [\ R_s \quad L_s\ ]^T \\ d_1(n) = [\ u_{d1} \quad u_{d2}\ ]^T \\ u_1^T(n) = \begin{bmatrix} i_{d1} & \frac{i_{d2}-i_{d1}}{T_s} - \omega_{e1} i_{q1} \\ i_{d2} & \frac{i_{d3}-i_{d2}}{T_s} - \omega_{e2} i_{q2} \end{bmatrix} \end{cases} \quad (5)$$

where $\hat{w}$ is the branch weight matrix, *d* is the expected response matrix, and u^T is the branch input matrix.

Step 2: Continue to identify ψ_f by treating R_s and L_s as known quantities. The voltage equations used for identification are as follows:

$$u_{q1} - \omega_{e1} L_s i_{d1} - R_s i_{q1} - \frac{L_s}{T_s}(i_{q2} - i_{q1}) = \omega_{e1}\psi_f + \zeta_3. \quad (6)$$

According to the RLS algorithm, the identification value of ψ_f can be obtained in real time according to the definition of the following formula:

$$\begin{cases} \hat{w}_2(n) = \psi_f \\ d_2(n) = u_{q1} - \omega_{e1} L_s i_{d1} - R_s i_{q1} - \frac{L_s}{T_s}(i_{q2} - i_{q1}) \\ u_2^T(n) = \omega_{e1}. \end{cases} \quad (7)$$

The flowchart of parameter identification algorithm for PMSM presented in this article is shown in Fig. 3. The resistance and inductance identification algorithm can be executed at a relatively fast speed, while the flux linkage identification algorithm can be executed at a relatively slow speed to save processor resources and meet the requirements of industrial production.

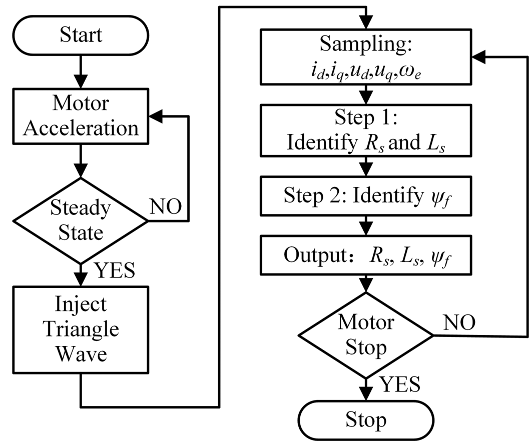

Fig. 3. Flowchart of parameter identification algorithm.

TABLE I
MAIN PARAMETERS OF SIMULATION AND EXPERIMENT

Parameter name	Value
Rated DC bus voltage / U_{dc}	20 V
Rated current / I_s	30 A
Rated speed / n_N	10 000 r/min
Polar logarithms / P_r	1
Stator resistance / R_s	0.025 Ω
Stator inductor / L_s	12 μH
Flux linkage / ψ_f	0.7 mWb
Switching frequency / f_{sw}	20 kHz
Sampling period / T_s	1×10^{-4} s
Triangular wave period / T_{tr}	2.5×10^{-3} s
Triangular wave amplitude / A_{tr}	1.75 A
Triangular wave DC offset / D_{tr}	0.4 A

III. EXPERIMENTAL RESULTS

In order to study the influence of triangular wave injection and current differential term on parameter identification results, and to verify the feasibility of the method in Section II, the proposed method and three comparison groups are experimented in this section.

A. Comparisons and Parameters of Experiment

In order to study the influence of triangular wave injection and current differential term on the parameter identification results, the following three comparison groups are set up.

1) *Comparison group 1:* Neither triangular wave nor current differential term is introduced.
2) *Comparison group 2:* The current differential term is introduced, but the triangular wave is not injected.
3) *Comparison group 3:* Injection of triangular wave, but no current differential term is introduced.

The main parameters of experiment are shown in Table I.

B. Analysis of Experiment

Furthermore, an experimental verification platform is built, as shown in Fig. 4, and the platform is mainly composed of personal computer, dc source, control source, inverter, motor, and oscilloscope.

Experimental waveforms of the motor speed and current values on the *d*- and *q*-axes during the entire identification process is shown in Fig. 5. It can be seen from Fig. 5 that

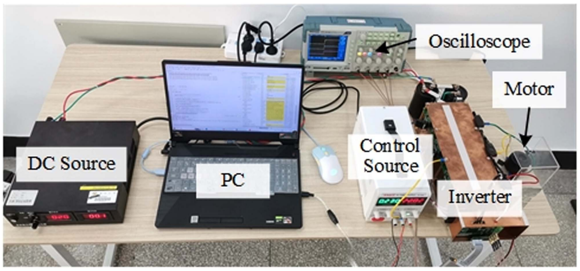

Fig. 4. Experimental platform.

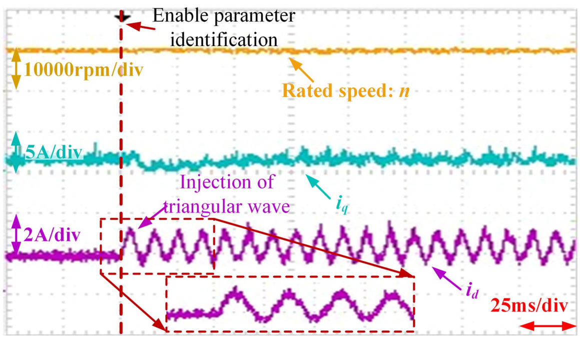

Fig. 5. Experimental waveform of rotational speed and current values on the d- and q-axes during identification process.

TABLE II
IDENTIFICATION ACCURACY OF FOUR METHOD (EXPERIMENT)

	Comparison group 1	Comparison group 2	Comparison group 3	Proposed method
E_{Rs} / %	Failed	Failed	2.4000	1.6000
E_{Ls} / %	Failed	8.8775	Failed	5.7167
$E_{\psi f}$ / %	7.8571	12.4714	5.2857	6.6857

when the motor reaches steady state, injecting a triangular wave into the i_d does not cause significant speed and i_q fluctuations, that is, the injection of the triangular wave does not have a significant impact on the operation of the motor. This confirms the robustness and resilience of the proposed technique.

Experimental results of the proposed method and three comparison groups are shown in Fig. 6 and Table II. Considering that the temperature rise of the motor is not high when the experiment is done in this article, the fluctuation range of the motor parameters is very small, and the nominal values in the Fig. 6 are all measured and calculated in the case of room temperature when the motor is stationary. It is found that the proposed method can successfully identify the resistance, inductance, and flux linkage, and the identification accuracy is very high. For comparison group 1, the current differential term and triangle wave are not introduced, so the identification model is not accurate enough and has the rank-deficient problem in a steady state, which leads to the failure of the identification of resistance and inductance. For comparison group 2, due to the introduction of the current differential term, the inductance can be successfully identified, but the value of the resistance has not yet been successfully identified. For comparison group 3, the rank-deficient problem of the model is improved and the SNR with R_s term is increased because of the injection of triangular wave, so the resistance can be identified successfully, but the inductance cannot be identified at the same time.

The proposed method successfully identifies the resistance, inductance, and flux linkage. However, there is ripple content in

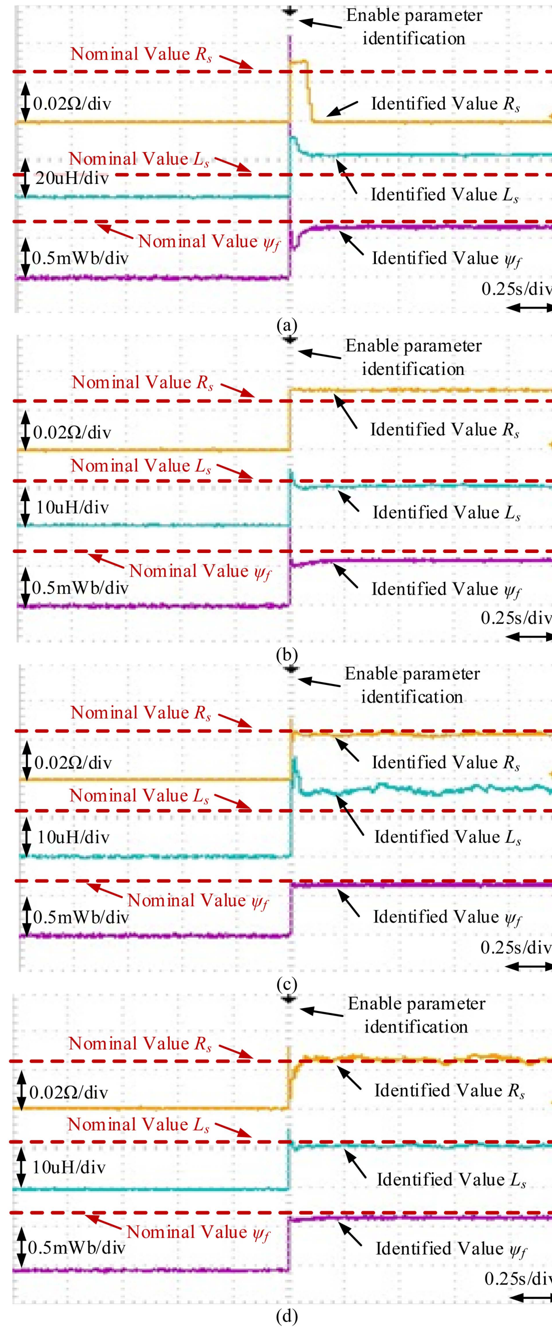

Fig. 6. Experimental results of four methods. (a) Identification results of comparison group 1. (b) Identification results of comparison group 2. (c) Identification results of comparison group 3. (d) Identification results of proposed method.

R_s and L_s, and the ψ_f value is slightly lower than the nominal value. This is because the motor parameter identification method proposed in this article is based on the continuous domain model method, the switching tube dead time will have an impact on the motor control, excessive dead time may result in insufficiently accurate modeling of the control motor, which affects the identification effect of the motor parameters.

In order to further confirm the effect of dead time on the proposed parameter identification method, experiments were carried out at different dead times, and the experimental comparison waveforms are shown in Fig. 7. It is found that the

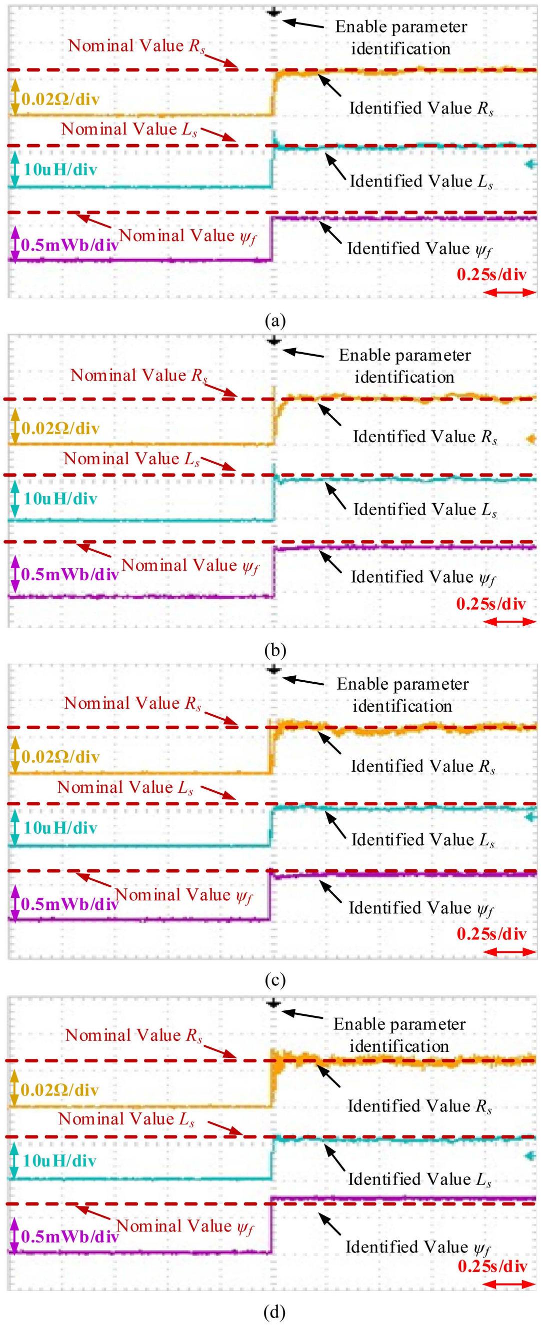

Fig. 7. Experimental waveforms with different dead times. (a) Dead time is set to 0.25 μs. (b) Dead time is set to 0.5 μs. (c) Dead time is set to 0.75 μs. (d) Dead time is set to 1 μs.

ripple content of R_s increases significantly with the increasing dead time, the identification result of ψ_f increases gradually, and the identification result of L_s does not produce a large change relative to the first two parameters.

To sum up, injecting triangle wave can solve the rank-deficient problem and improve the SNR with R_s term, and the current differential term can improve the accuracy of the identification model and the SNR with L_s term. The identification method proposed in this article combines the above two measures, so it can identify R_s, L_s, and ψ_f at the same time, and obtain a good accuracy. At the same time, it has been confirmed that the accuracy of motor parameter identification is affected by dead time.

IV. Conclusion

In this article, the issues, such as model accuracy, rank-deficient, and the incompletely observable in the steady-state operation of PMSM, are analyzed. Therefore, a parameter identification method based on biased triangular wave injection and current differential term is proposed in this article. First, the current differential term is introduced to improve the accuracy of the model. Second, the rank-deficient problem is solved by using the two sets of sampling results as identification equations. Finally, by injecting triangular wave into *d*-axis current, the problem that motor cannot be fully observed in the steady-state operation is solved. Furthermore, three comparison groups are set up to study the influence of triangular wave injection and current differential term on the parameter identification. The experimental results show that the injected triangular wave can solve the rank-deficient problem and improve the SNR of R_s term, and the current differential term can improve the accuracy of the identification model and the SNR of L_s term. The identification method proposed in this article combines the above two measures, so it can identify R_s, L_s, and ψ_f at the same time, and obtain a good accuracy. At the same time, it has been confirmed that the accuracy of motor parameter identification is affected by the dead time.

References

[1] M. S. Rafaq and J.-W. Jung, "A comprehensive review of state-of-the-art parameter estimation techniques for permanent magnet synchronous motors in wide speed range," *IEEE Trans. Ind. Informat.*, vol. 16, no. 7, pp. 4747–4758, Jul. 2020.

[2] N. Y. A. Qamar and C. J. Hatziadoniu, "Cancelation of torque ripples in PMSM via a novel minimal parameter harmonic flux estimator," *IEEE Trans. Power Electron.*, vol. 34, no. 3, pp. 2553–2562, Mar. 2019.

[3] Q. Wang et al., "An offline parameter self-learning method considering inverter nonlinearity with zero-axis voltage," *IEEE Trans. Power Electron.*, vol. 36, no. 12, pp. 14098–14109, Dec. 2021.

[4] S. J. Underwood and I. Husain, "Online parameter estimation and adaptive control of permanent-magnet synchronous machines," *IEEE Trans. Ind. Electron.*, vol. 57, no. 7, pp. 2435–2443, Jul. 2010.

[5] K. Liu, Z. Q. Zhu, and D. A. Stone, "Parameter estimation for condition monitoring of PMSM stator winding and rotor permanent magnets," *IEEE Trans. Ind. Electron.*, vol. 60, no. 12, pp. 5902–5913, Dec. 2013.

[6] K. Liu and Z. Q. Zhu, "Position-offset-based parameter estimation using the adaline NN for condition monitoring of permanent-magnet synchronous machines," *IEEE Trans. Ind. Electron.*, vol. 62, no. 4, pp. 2372–2383, Apr. 2015.

[7] K. Liu and Z. Q. Zhu, "Quantum genetic algorithm-based parameter estimation of PMSM under variable speed control accounting for system identifiability and VSI nonlinearity," *IEEE Trans. Ind. Electron.*, vol. 62, no. 4, pp. 2363–2371, Apr. 2015.

[8] Y. Yu et al., "Full parameter estimation for permanent magnet synchronous motors," *IEEE Trans. Ind. Electron.*, vol. 69, no. 5, pp. 4376–4386, May 2022.

[9] J. Zhang, F. Peng, Y. Huang, Y. Yao, and Z. Zhu, "Online inductance identification using PWM current ripple for position sensorless drive of high-speed surface-mounted permanent magnet synchronous machines," *IEEE Trans. Ind. Electron.*, vol. 69, no. 12, pp. 12426–12436, Dec. 2022.

[10] S. Ye and X. Yao, "A modified flux sliding-mode observer for the sensorless control of PMSMs with online stator resistance and inductance estimation," *IEEE Trans. Power Electron.*, vol. 35, no. 8, pp. 8652–8662, Aug. 2020.

[11] C. Wu, Y. Zhao, and M. Sun, "Enhancing low-speed sensorless control of PMSM using phase voltage measurements and online multiple parameter identification," *IEEE Trans. Power Electron.*, vol. 35, no. 10, pp. 10700–10710, Oct. 2020.

[12] Y. Yao, Y. Huang, F. Peng, and J. Dong, "Position sensorless drive and online parameter estimation for surface-mounted PMSMs based on adaptive full-state feedback control," *IEEE Trans. Power Electron.*, vol. 35, no. 7, pp. 7341–7355, Jul. 2020.